JMEPEG (2007) 16:626–634
DOI: 10.1007/s11665-007-9110-7

1059-9495/$19.00

Electrical and Physical Characterization of Bulk Ceramics and Thick Layers of Barium Titanate Manufactured Using Nanopowders

Dinh Quang Nguyen, Thierry Lebey, Philippe Castelan, Vincent Bley, Madona Boulos, Sophie Guillemet-Fritsch, Céline Combettes, and Bernard Durand

(Submitted September 8, 2005; in revised form June 5, 2006)

Fine powders of $BaTiO_3$ are synthesized by hydrothermal processing at 250 °C for 7 h. Two different starting mixtures were used, $TiCl_3 + BaCl_2$ and $TiO_2 + BaCl_2$. The size of the resulting crystallites was close to 20 nm in both cases. The powders were formed into ceramic pellets or thick layers. The samples were characterized for microstructure and electrical permittivity. The impact of the microstructure on the electrical properties is emphasized, and is correlated to the powder characteristics and the powder realization process.

Keywords barium titanate, dielectric properties, hydrothermal synthesis, ceramic, thick layer

1. Introduction

Integration of passive components in power electronics is one of the most challenging topics, in which a material must perform more than one function. In this regard, high-permittivity materials have a key role to play. Among them, barium titanate appears to be a good candidate, thanks to its high-permittivity value and low losses. It has been used for a long time in electric and electronic equipment (Ref 1, 2), telecommunications, and other applications in which the materials are subjected to substantial changes in temperature, frequency, and voltages (Ref 1-5). Barium titanate is widely used in the manufacture of multilayer capacitors (MLC) in which the ceramic layers (some tens of micrometer) are intertwined with inner electrodes. The goal of this article is to enhance the electrostatic capacitance using at the same time a large surface and a high-permittivity material. Generally speaking, two forms of barium titanate are in use: (1) bulk ceramics (thickness more than 1 mm) and (2) thick layer ceramics whose thicknesses vary from 10 μm to 100 μm. Bulk ceramics of $BaTiO_3$ may be prepared easily by conventional method, pressing powders in a mold and firing them at a temperature between 1200 and 1300 °C (Ref 3, 5, 6).

Dinh Quang Nguyen, Thierry Lebey, Philippe Castelan, and **Vincent Bley,** Laboratoire de Génie Electrique de Toulouse (LGET), Bât. 3R3, Université Paul Sabatier, 118, route de Narbonne, 31062, Toulouse Cedex 04, France; **Madona Boulos, Sophie Guillemet-Fritsch, Céline Combettes,** and **Bernard Durand,** Centre Inter-Universitaire de Recherche et d'Ingénierie des Matériaux (CIRIMAT), Bât. 2R1, Université Paul Sabatier, 118, route de Narbonne, 31062, Toulouse Cedex 04, France. Contact e-mail: lebey@lget.ups-tlse.fr.

Thin layers may be deposited on substrates by various techniques, i.e., evaporation, sol-gel, or sputtering. In these techniques, typical layer thicknesses range from 0.1 μm to a few μm (Ref 7, 8). When for thicker layers are desired (>10 μm) the preceding methods are no longer used; instead, dip coating, spin coating, and chemical vapor deposition techniques with limited success for thick coating are used. Other techniques, such as doctor blade tape casting or screen printing are relatively simple and convenient methods, producing up to hundreds of micrometer (Ref 7, 9, 10). These techniques, however, the preparation require of a slurry which may inhibit the final properties of the layers, if its rheological properties are not appropriate. These layers are then fired at a temperature ranging from 850 up to 1200 °C, depending on the kind of slurry and the materials used to make the electrodes.

The starting point is in any fabrication process always the powder synthesis. In a previous study (Ref 11), two different routes for the manufacture of powders were investigated: the classical solid/solid method and a soft chemistry method: the co-precipitation. The co-precipitation method is based on the formation of a mixed-metal complex which is thermally decomposed at a temperature above 500 °C. High-purity $BaTiO_3$ is prepared using the Pechini-type reaction, yelding nanosized and well-crystallized cubic $BaTiO_3$. Complete decomposition of oxalate complex that is produced, however, takes a very long time.

When making ceramic pellets, the soft chemistry route led to higher permittivity values than the classical solid/solid route. This result was attributed to a better control of the quality of raw material powders including their grain size.

In this work, another soft chemistry route is used for the synthesis of barium titanate: the hydrothermal synthesis. The hydrothermal synthesis is one of the best methods for producing metal oxide particles. It has many advantages such as highly crystalline particles, low-cost starting materials, low-temperature treatment, and simple procedure. Consequently, it allows a better control of the powder properties.

Two titanium sources were used with the following chemical reactions:

Table 1 Specific surface area S_w, crystallite size d_x and particle grain size d_{BET} of the $BaTiO_3$ powders synthesized by hydrothermal method

Ti precursor	Synthesis temperature (°C)	S_w (m^2/g)	d_x (nm)	d_{BET} (nm)
$TiCl_3$	250	13.5	21	74
TiO_2	250	13.0	21	74

d_x was calculated from the broadening of the XRD peak using the Scherrer formula $d_x = 0.94\lambda/\beta\cos\theta$, S_w was measured by BET method and d_{BET} was calculated by the formula $d_{BET} = 6/S_w\ \rho$(ρ: volume mass of powder)

TiO_2 starting material: $TiO_2 + BaCl_2 + 1/2\ O_2 \rightarrow BaTiO_3 + 2Cl^-$

$TiCl_3$ starting material:

$$4TiCl_3 + O_2 + 2H_2O \rightarrow 4TiO^{2+} + 4H^+ + 12Cl^-$$
$$TiO^{2+} + 1/2\ O_2 \rightarrow TiO_2$$
$$TiO_2 + BaCl_2 + 1/2\ O_2 \rightarrow BaTiO_3 + 2Cl^-$$

In the following, the influence of both the methods and the titanium sources on the final properties of two different kinds of samples (ceramic pellets and thick layers) are presented and discussed.

2. Experimental

2.1 Preparation of $BaTiO_3$ Powders

The starting materials were barium chloride ($BaCl_2.2H_2O$, Prolabo 99%), titanium chloride ($TiCl_3$, Prolabo, d = 1.20, % min = 15%), and titanium oxide (TiO_2, anatase, Rhodia). $TiCl_3$ was preferred over $TiCl_4$ since it is less sensitive to moisture. Moreover, solid $TiCl_3$ can be easily dissolved in water and the hydrolysis prevented by acidification. An acid solution of $TiCl_3$ is also easier to handle than liquid $TiCl_4$. Aqueous solutions of barium and titanium were obtained by mixing 0.015 mol $TiCl_3$ or TiO_2 and 0.024 mol $BaCl_2.2H_2O$ in deionized water.

The formation of $BaTiO_3$ was promoted by an initial precursor molar ratio Ba/Ti = 1.6. However, it is assumed that the loss of some Ba^{2+} ions during the fabrication process will occur. It leads to a Ba/Ti ratio in the final product which is close to unity. In fact, x-ray diffraction spectra, presented later, showed only $BaTiO_3$ peaks, and no other Ti species were found.

The pH of the solution was raised up to 13.5 by adding a well-stirred solution of KOH. The suspension was transferred into a cylindrical autoclave (Paar, Teflon lined stainless steel 600 ml, filled at 2/3 of its volume). The autoclave was put inside a preheated regulated oven, and the reaction was heated for 7 h at 250 °C under autogenous pressure (5-39 bars). After cooling to room temperature, the water insoluble reaction product was washed with a solution 0.1 M HCl to remove the $BaCO_3$, which was present with $BaTiO_3$ at the end of the hydrothermal treatment. The powder is then filtered, washed several times with distilled water, and oven dried at 110 °C for 24 h.

The powder properties were carefully controlled. The structure was identified using x-ray diffractometry (Siemens D 501 diffractometer equipped with a SiLi detector, $\lambda_{CuK\alpha}$ = 1.5418 Å) and microstructural studies were performed using electron microscopy (Jeol JSM 6700F SEM-FEG).

The specific surface of the powder was also measured by nitrogen desorption according to the BET method (Micromeritics Desorb 2300A/Flow sorb II 2300). Raman investigations were carried out by means of DiLor XY Micro Raman Spectrometer equipped with a Princeton Instruments LN/CCD detector. Electron Paramagnetic Resonance (EPR) was used to detect the presence of Ti^{3+} in samples using a Bruker ESP 300 spectrometer operating at X-band frequency and 100 kHz field modulation (Ref 3). The most relevant physical parameters are summarized in Table 1.

2.2 Preparation of the $BaTiO_3$ Pellets

The powders were first pressed in a metal mold under 250 MPa to a thickness ranging from 1.5 mm to 2 mm and the surface is 20 mm^2. The pellets were then sintered in air at 1250 °C for two dwell times, 10 and 20 h. The heating rate is fixed at 80 °C/h. After cooling at room temperature, the ceramics were metalized by screen printing a silver mixture on the two faces of the ceramics, then annealing them at 750 °C.

2.3 Thick Layers

For thick-layer realization, the slurry of $BaTiO_3$ was carefully prepared since its quality has a large impact on the final product. The powders were fired at 800 °C to reduce the water content and to decrease the specific surface down to about 7 m^2/g. A ball mill was used to mix $BaTiO_3$ powders and an additive solution constituted of adhesive organic, a solvent and a dispersant prepared by stirring for 48 h. The optimum viscosity of the slurry is 250 Pa.s.

Layers of $BaTiO_3$ material were then deposited on a substrate of alumina. A platinum (Pt) electrode was used for the lower electrode, and a silver electrode for the upper one. These electrodes were deposited using the same process used to apply electrodes on the $BaTiO_3$ layers. Commercial products from dmc^2 (576402 platinum and AgPdPt T 5365) were used to make the electrodes. The layer of Pt was fired at a temperature of 850 °C in air. It was used as an electrode, since it is able to withstand the high temperature (1250 °C) which associated the sintering process. After deposition and before sintering, the $BaTiO_3$ layers were heated at 450 °C to burn the adhesive organic part of the slurry and to remove the solvent. The samples were then sintered at 1200 °C in air for 10 h. The thermal treatment achieved at 450 °C helps to avoid internal stresses during sintering, which could lead to mechanical fracture.

Electrical characterization was performed in the 20 Hz-10 MHz range on the different types of samples was conduced with a HP 4284A precision LCR meter and a Hewlett Packard HP 4194 Impedance/Gain-Phase Analyzer. Samples were placed in an oven (HERAEUS HT7010) and measurements

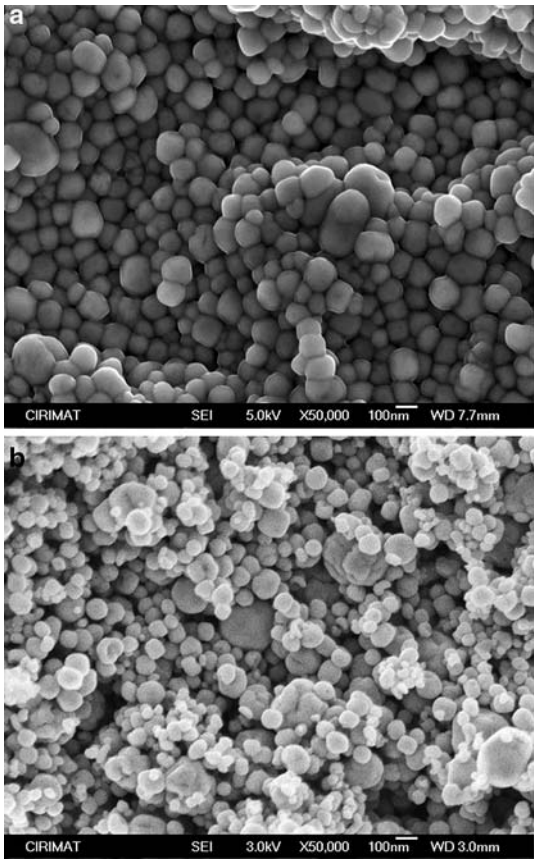

Fig. 1 SEM-FEG photomicrograph of $BaTiO_3$ powders prepared from $TiCl_3$ (a) and TiO_2 (b) at 250 °C

taken between room temperature and 150 °C in controlled increments.

3. Results and Discussion

3.1 Powder Characterization

Whatever the titanium source ($TiCl_3$ or TiO_2), and for a reaction temperature of 250 °C, chemical analyses showed that the molar ratio Ba/Ti was very close to one, (Ba/Ti ~ 1). As mentioned previously, the loss of some Ba^{2+} ions during the elaboration process is assumed, and it leads to a Ba/Ti ratio in the final product close to one. X-ray diffraction spectra had only $BaTiO_3$ peaks, with no other Ti species were found. The morphology and the particle size of the $TiCl_3$ and TiO_2 starting powders obtained at 250 °C was determined by scanning electron microscopy, and are shown in Fig. 1(a) and (b). At this stage, their morphology is not very different. The average crystallite size of the powder grains, determined from x-ray diffraction data (Fig. 2), is about 20 nm for $TiCl_3$ (yellow) and TiO_2 (white) (Table 1). The mean size of the crystallites, d_x, was calculated from the broadening of the XRD peaks using the Scherrer formula. According to x-ray diffraction analysis, the structure of both powders is perovskite type. It did not contain impurities (Ref 3).

Raman spectra indicated the coexistence at room temperature of two $BaTiO_3$ different phases: tetragonal and cubic

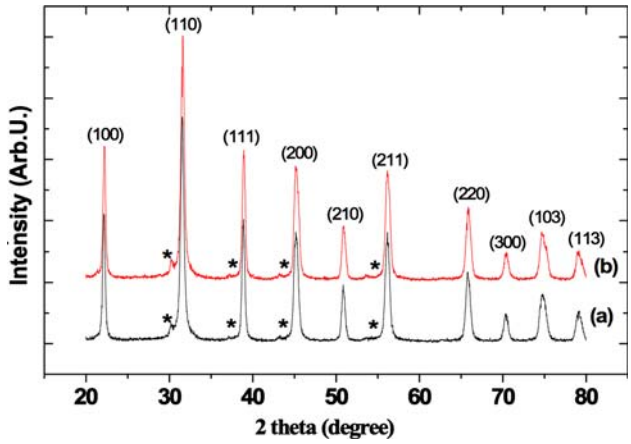

Fig. 2 X-ray diffraction patterns of $BaTiO_3$ powders prepared from $TiCl_3$ (a) and TiO_2 (b) at 250 °C. * The small peaks are fluorescence signals coming from pollution of the copper anti-cathode by tungsten of the filament

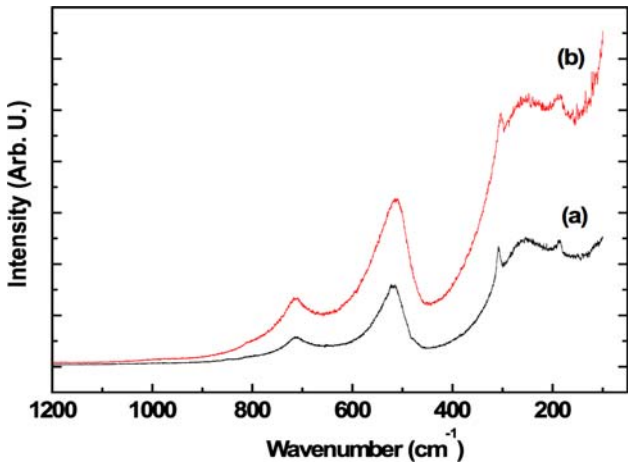

Fig. 3 Raman spectra of $BaTiO_3$ powder synthesized from $TiCl_3$ (a) and TiO_2 (b) at 250 °C

(Fig. 3). $BaTiO_3$ exhibits two large bands, at 520 and 716 cm^{-1} for tetragonal with nearly the same intensities and another larger band at 707 cm^{-1} for cubic polymorph (Ref 3, 12, 13). No EPR signal was observed for the samples synthesized from TiO_2. The EPR spectrum of a sample prepared using $TiCl_3$ as precursor is shown in Fig. 4. The signals near 3500 G are characteristic of isolated Ti^{3+} ions. It is known that Ti^{3+} is unstable in the presence of atmospheric oxygen and oxidizes into Ti^{4+}. The small amount of Ti^{3+} detected in the powders prepared from $TiCl_3$ indicate that complete oxidation of Ti^{3+} to Ti^{4+} during the synthesis did not occur.

3.2 Properties of Bulk Ceramics and Thick Layers

In the case of ceramic pellets, only the tetragonal $BaTiO_3$ phase is evident (Fig. 5), which is the common phase observed in such cases (Ref 14). The microstructure of bulk $BaTiO_3$ ceramics sintered at 1250 °C for 10 h is shown in Fig. 6(a) and 7(a) for $TiCl_3$- and TiO_2-based materials, respectively. Abnormal grain growth is noticed for both the samples. The microstructure of these ceramics is bimodal, constituted of

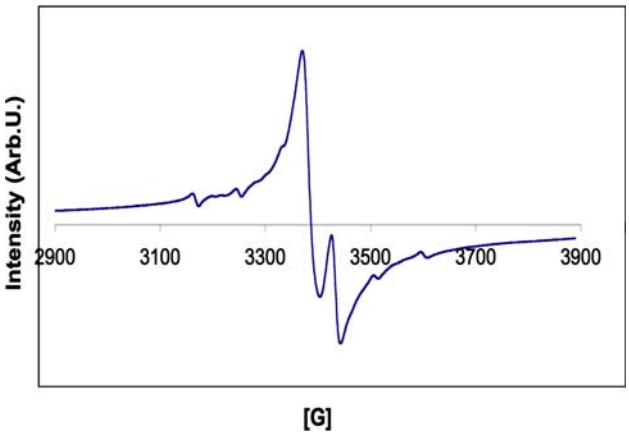

Fig. 4 EPR spectra of Ti^{3+} in $BaTiO_3$ synthesized using $TiCl_3$ as precursor

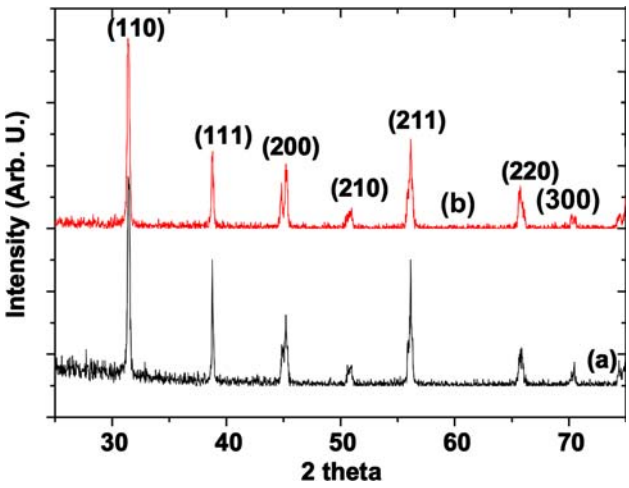

Fig. 5 X-ray diffraction patterns of $TiCl_3$ based ceramic (a) and TiO_2 based ceramic (b), sintered at 1250 °C for 10 h

large (up to 60 μm) angular grains growing in a fine-grained (1 μm) matrix. The density values of sintered bulk ceramic are reported in Table 2. The density of samples sintered during 10 h reached 94.5% of the theoretical value. It is well known that the increase of the dwell time may have an effect on the final density. In another work (Ref 3), the densification reached 99.8% in some cases (dwell time 20 h at 1250 °C). The longer dwell time also modifies the grain size and its distribution, especially for powders prepared from $TiCl_3$. Samples of powders prepared using TiO_2 show fewer grains in the fine-grained matrix. The difference in the ceramic microstructures prepared from powders synthesized using $TiCl_3$ or TiO_2 could be explained by the presence of Ti^{3+} in initial powders. It is well known that the presence of titanium in the material causes grain growth and could be the reason why we observe more large grains in the $TiCl_3$-based ceramic.

The thick layers sintered at 1200 °C were homogeneous in thickness, as shown by the cross-section micrograph (Fig. 8a, b). The thicknesses of each layers, estimated from SEM micrographs, are roughly: 7 μm for the upper Ag electrode, 40 μm for the $BaTiO_3$ layer, 10 μm for the Pt bottom electrode, and 500 μm for the substrate layer Al_2O_3. The grain-size

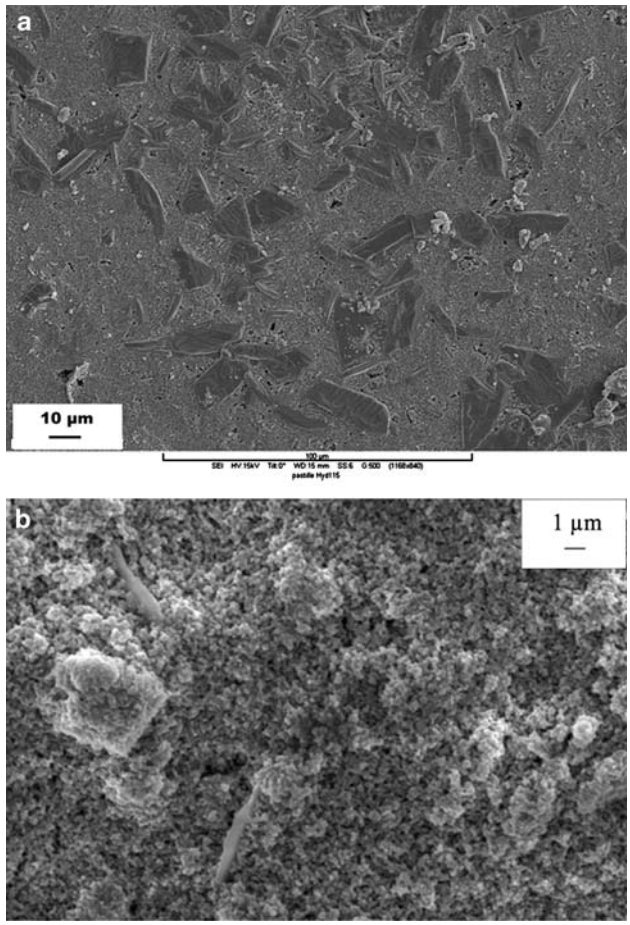

Fig. 6 SEM pictures of $BaTiO_3$ materials prepared from $TiCl_3$ and sintered at 1250 °C for 10 h, (a) ceramics pellets (b) thick layers

distribution is homogenous, ranging between 0.2-0.5 μm (for the $TiCl_3$ starting powders) and 0.5-1 μm (for the TiO_2 starting powders), as shown in Fig. 6(b) and 7(b), respectively. In both cases, the grain size of the $BaTiO_3$ layer is less than 1 μm. No abnormal grain growth has been noticed in this case. As reported in the literature for $BaTiO_3$ thick layers (Ref 15, 16), the grain growth was attributed to the presence of impurities; such as Si, Al, or Na (20-100 ppm); present in commercial undoped $BaTiO_3$ powders obtained by solid-state reaction. In the present case, the sintering treatment has been performed at a lower temperature; 1200 °C (1250 °C for bulk ceramics). Obviously some porosity remains, as shown on the surface and in the cross section of the layer (Fig. 6b, 7b and 8b). However, it must be noticed that no glass frit was added to the $BaTiO_3$ powder as is usually the case in industrial practice. It is important to note that neither cracks nor delaminations are observed, indicating a relatively good compatibility between the different layers. Finally, the quality of the layer is rather acceptable (Fig. 8). A similar kind of work was performed by Yoon and Lee (Ref 15, 16), who tested a series of different binders. They found that parameters such as the density and the dielectric permittivity depended significantly on the type of powders used and the sintering conditions, rather than on the binder type.

The results of the electrical measurements will be discussed next. Changes in both the real and imaginary part the of complex permittivity [$\varepsilon^*(\omega) = \varepsilon'(\omega) - j\varepsilon''(\omega)$, where $\omega = 2\pi f$,

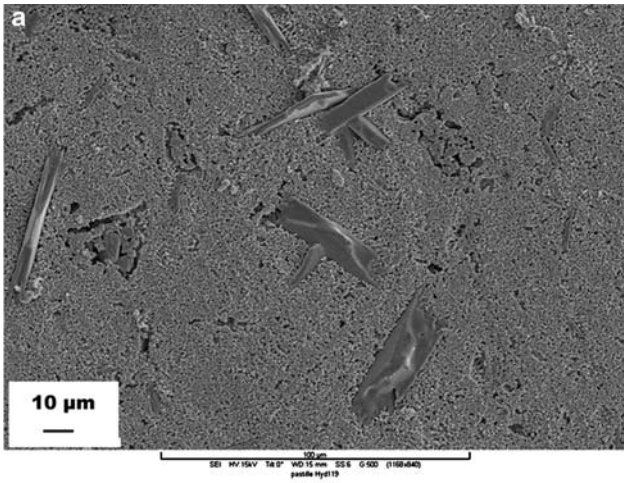

Fig. 7 SEM pictures of $BaTiO_3$ materials prepared from TiO_2 and sintered at 1250 °C for 10 h, (a) ceramics pellets and (b) thick layers

Table 2 Density (%d_{th}) of ceramic after sintering at 1250 °C during 10 h

Ti precursor	Synthesis temperature (°C)	Dwell time (h)	% d_{th}
$TiCl_3$	250	10	94.5
TiO_2	250	10	92.2

f is the frequency] are measured at room temperature as a function of frequency, give results as shown in Fig. 9 for the ceramic pellets and thick layers samples when the frequency increases. The permittivity of bulk ceramic samples is higher than that of thick layers of barium titanate. Moreover, the permittivity of bulk ceramics stays constant in the measured frequency range, but for thick layers samples, it tends to decrease as the frequency rises in the MHz range.

Figure 10(a) and (b) represent the changes in the permittivity values at different frequencies versus the temperature for both bulk ceramics and the thick layers prepared under the same conditions, and for different kinds of starting powders.

The main electrical properties are summarized in Table 3 and are the following:

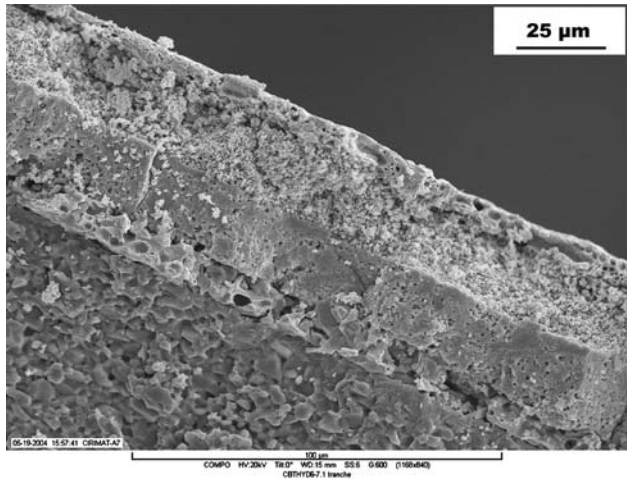

Fig. 8 SEM pictures of a cross section of the thick layer sample (TiO_2-based ceramics) showing the different layers

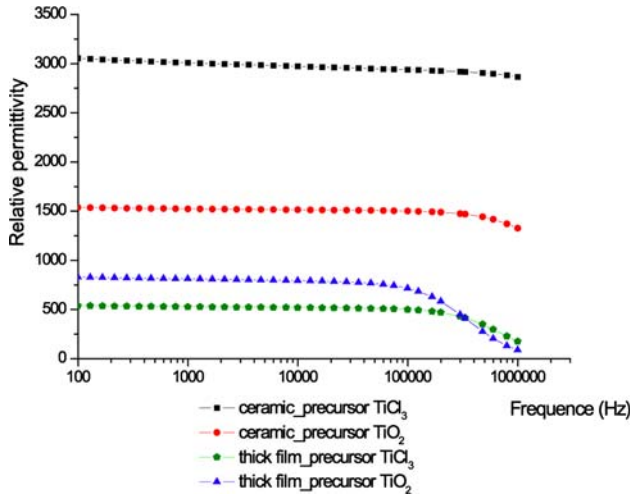

Fig. 9 Changes in the permittivity values versus the frequency for the two starting titanium sources and for the two forms of materials

- The Curie temperature (T_c) depends on the nature of the starting powder. For bulk ceramic samples, T_c is close to 110 °C and 125 °C, respectively for $TiCl_3$- and TiO_2-based powders. For thick layer/TiO_2-based powders samples, T_c is the same (125 °C) whereas a clear transition is not observed for the $TiCl_3$-based samples. A slight decrease of the permittivity is observed at a temperature larger than 90 °C. The transition is sharp for bulk ceramics/TiO_2 based powders samples, whereas it is wider for the thick layer/TiO_2 samples.
- The permittivity value depends on the nature of the sample, with highest values obtained for the pellets. This difference is observed in all types of materials over the whole temperature range. For samples made using TiO_2-based sample layers, the permittivity at room temperature is 800 and reaches 1350 at T_c. This value is a little higher than the value of 1100 reported by Stojanovic et al. (Ref 7, 8) for a two-layer sample of thickness 50 µm.
- The maximum value at room temperature is obtained for the TiO_2 based bulk ceramic, with a value larger than 1100 obtained at the Curie temperature.

– For thick layers of $BaTiO_3$ prepared from the $TiCl_3$ starting powders, a quasi-constant value (near 500) is obtained.

In order to have a deeper understanding of the properties of different types of the samples studied, the data may be plotted in an "Argand" diagram which results from the Cole-Cole model (Ref 17, 18).

According to this model, the complex permittivity may be written as:

$$\varepsilon^* = \varepsilon'(\omega) - j\varepsilon''(\omega) = \varepsilon_\infty + \frac{\varepsilon(0) - \varepsilon_\infty}{1 + (j\omega\tau_m)^\gamma} \quad 0 < \gamma = 1 - \frac{2\theta}{\pi} \leq 1 \tag{Eq 1}$$

Where $\varepsilon'(\omega)$ and $\varepsilon''(\omega)$ are the real and imaginary part of the permittivity, respectively, ε_∞ is the permittivity at the highest frequency f (when f tends to ∞), $\omega = 2\pi f$, $\varepsilon(0)$ is the permittivity at a frequency near 0, γ is an exponent, θ is the angle with respect to the semicircle center [radian], and τ_m is the average relaxation time [s] (see Fig. 11a for the definitions).

A least square method circular regression and experimental data (Ref 19, 20) are used to create the semi-circular plots shown in Fig. 11 and to determine θ. It is a simple and quick method to obtain unknown parameters with a functional dependence and estimate the uncertainty of these parameters. The angle θ is related to the distribution of relaxation time, being maximal when $\theta = \pi/2$, and minimum when $\theta = 0$ (case of Debye model). The logarithmic distributions of relaxation times ($f(s)$) (Fig. 11b) of bulk and thick layer ceramic materials are calculated by using the following equations (Ref 21-23):

$$f(s) = \frac{1}{2\pi}\frac{\sin(1-\gamma)\pi}{\cosh(\gamma s) - \cos(1-\gamma)\pi} = g_{\theta,\tau_m}(\tau) \tag{Eq 2}$$

where

$$s = \ln\left(\frac{\tau}{\tau_m}\right) \text{ and } \int_{\tau=0}^{+\infty} f(s)d\ln\tau = 1 \tag{Eq 3}$$

Then the average relaxation time τ_m is calculated as follows:

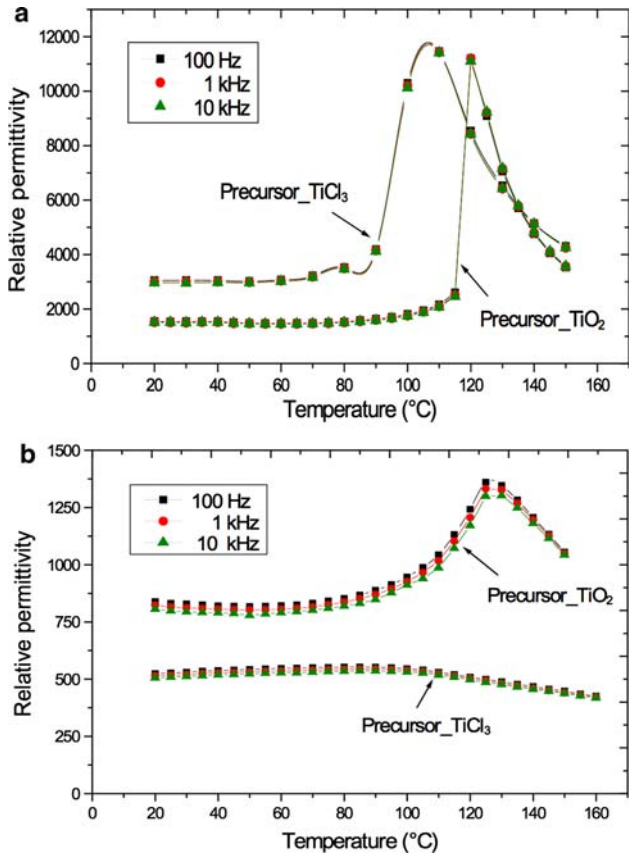

Fig. 10 Changes in the permittivity values versus the temperature for the two starting titanium sources and for the two forms of materials, (a) ceramic and (b) thick layers samples

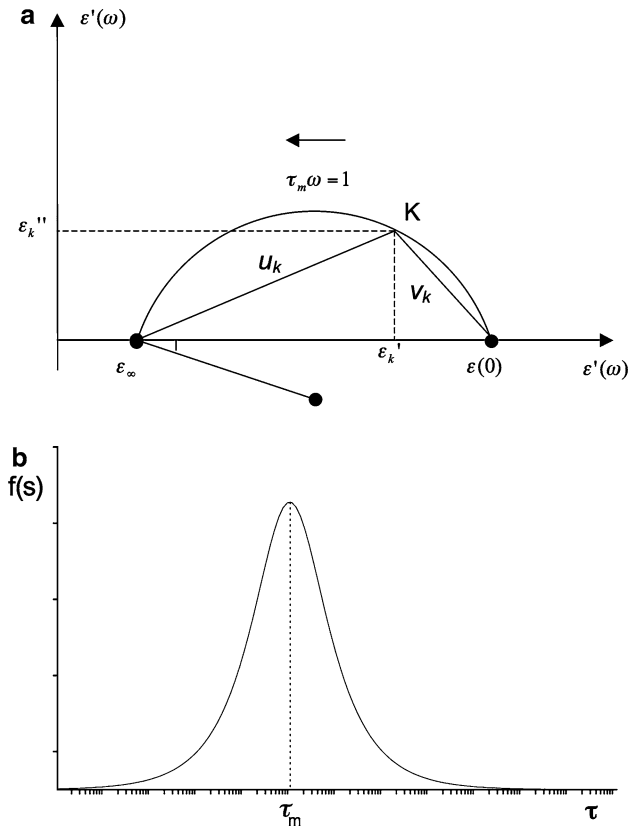

Fig. 11 Definition of the different parameters in a Cole-Cole plot

Table 3 Relative permittivity (ε′), loss dielectric (tg δ), and Curie (T_c) temperature of the $BaTiO_3$ ceramic pellets and thick layers prepared from "hydrothermal" powders

Sample type/starting salt	*T* (°C) and time (h) of sintering	ε′ (40 °C)	ε′ (*Tc*)	tg δ (40°C)	tg δ (*Tc*)	Tc (°C)
Ceramic /$TiCl_3$	1250/10	3007	11,432	0.00984	0.00238	110
Ceramic /TiO_2	1250/10	1520	11,200	0.00434	0.00526	125
Thick layer /$TiCl_3$	1200/10	537	553	0.01545	0.0184	90
Thick layer /TiO_2	1200/10	820	1360	0.01601	0.0093	125

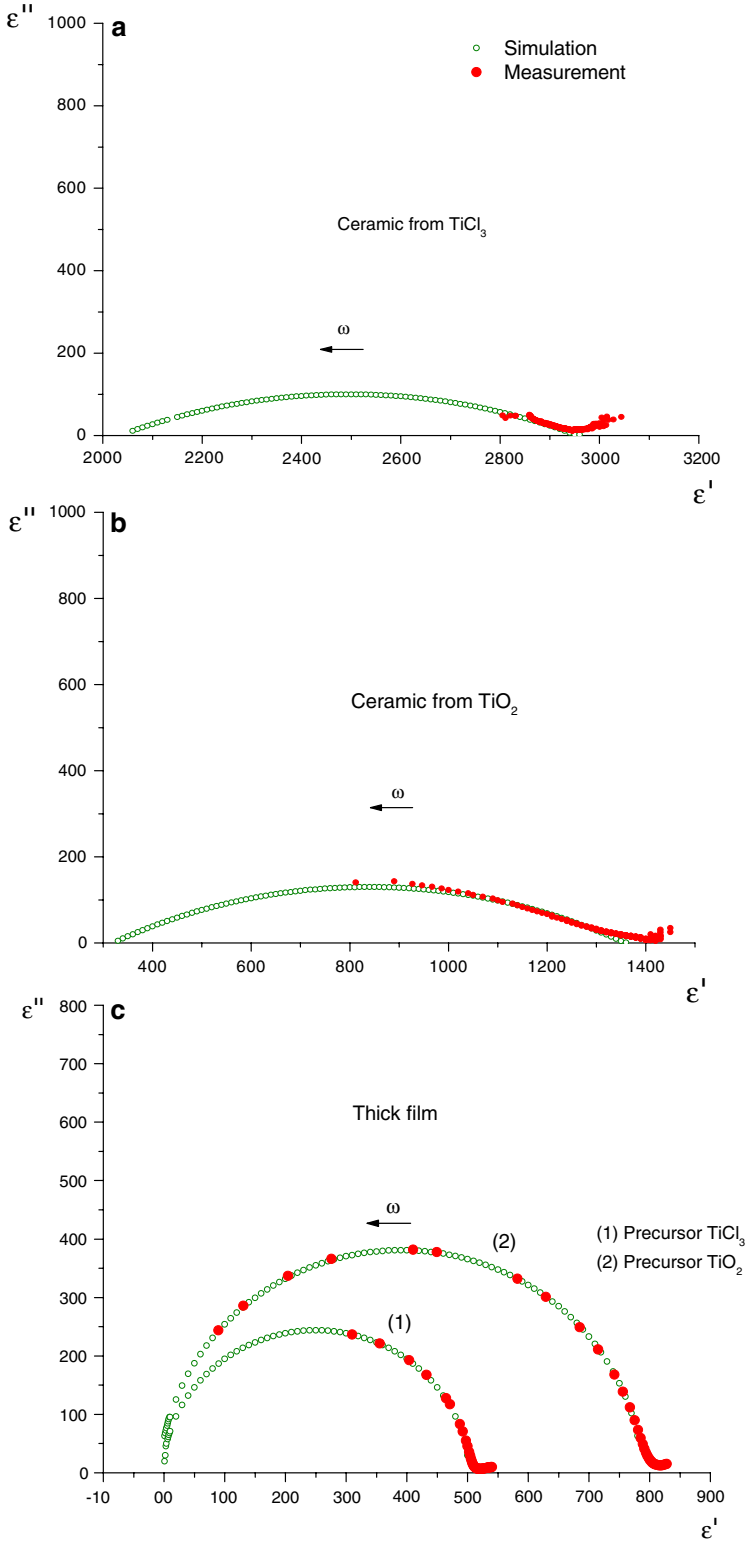

Fig. 12 Argand diagrams for the two starting titanium sources and for the two forms of materials, (a) ceramic pellets from $TiCl_3$, (b) ceramic pellets from TiO_2, and (c) thick layers from $TiCl_3$ (1) and TiO_2 (2)

$$\tau_m = \left[\prod_{k=1}^{n} \tau_{mk}\right]^{\frac{1}{n}} = \left\{\prod_{k=1}^{n} \frac{1}{\omega_k}\left[\frac{u_k}{v_k}\right]^{-\frac{1}{\gamma}}\right\}^{\frac{1}{n}} \qquad \text{(Eq 4)}$$

where $u_k = \sqrt{(\varepsilon'_k - \varepsilon_\infty)^2 + \varepsilon''^2_k}$ and $v_k = \sqrt{(\varepsilon(0) - \varepsilon'_k)^2 + \varepsilon''^2_k}$, and n is the number of measurement points on the arc diagram. ε'_k and ε''_k are the real and imaginary parts of the permittivity measured at point k corresponding to the frequency f_k.

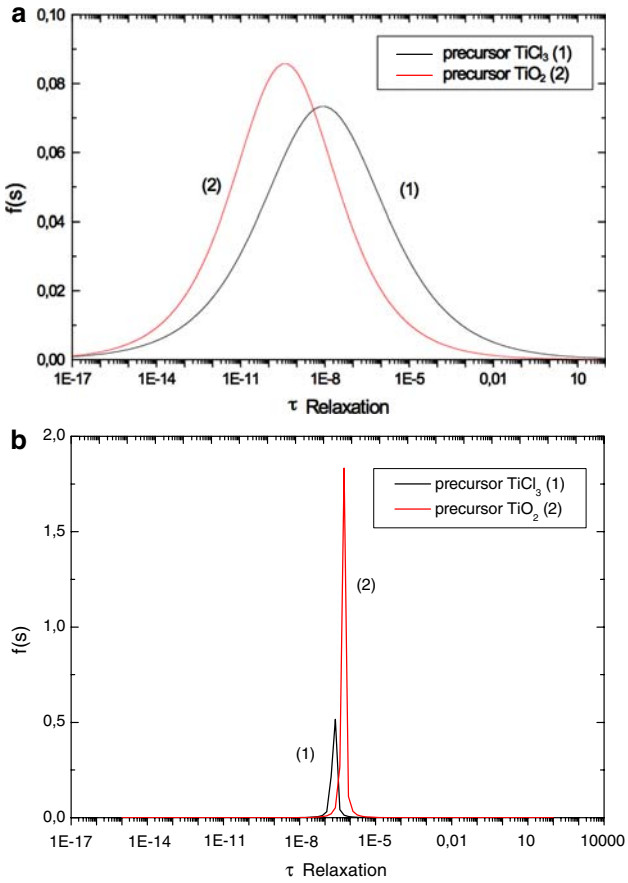

Fig. 13 Distribution of the relaxation times for the ceramic pellets (a) and thick layers (b) for the two starting precursors

Figure 12(a) through (c) present these plots for the ceramic pellets (a and b) and thick layer samples (c) prepared from TiO_2 and $TiCl_3$ powders, respectively. For the ceramic samples, the center of the semi circles in Fig. 12 has a negative ordinate. The angles θ calculated from Eq 1 are 1.0761 rad and 1.1387 rad for the ceramic samples prepared from TiO_2 and $TiCl_3$ powders, respectively whereas they are slightly different from zero for the thick layer samples (0.04 for TiO2 and 0.02 for $TiCl_3$). These results confirm that the structure of the ceramic pellets is less homogeneous than the structure of the thick layer ceramics (Ref 20, 23). This assumption is reinforced when plotting the distribution of relaxation times (Fig. 13). The distribution for the bulk samples is wider (Fig. 13a) than the one obtained for the thick layer samples (Fig. 13b), meaning a distribution of the relaxation times is associated with the type (and size) of the relaxing species (Ref 23, 24). The average values of τ_m are 2.2438×10^{-7} s and 5.2545×10^{-7} s for thick layers samples prepared from $TiCl_3$ and TiO_2 powders, respectively. For the pellets $TiCl_3/TiO_2$ samples, these values are 8.5731×10^{-9} s and 3.7699×10^{-10} s respectively and explain the results observed in Fig. 9 regarding the changes in permittivity of thick layers when the frequency is in the MHz range. The average relaxation time of dielectric thick layers is large, indicating that the inertia of the dipoles in the thick layers is larger than in the ceramic samples. Therefore, the time to achieve a complete polarization of dipole is longer. When the frequency increases, since the polarization is not completed, the total dipole vector along the axis parallel to the direction of the applied field is low. The material permittivity does not achieve the maximum value throughout the period of the frequency variation. This physical process is clearly pointed out in the expression giving the relationship between the permittivity and time of applied voltage t (Ref 18):

$$\varepsilon(t) = \varepsilon_\infty + (\varepsilon_s - \varepsilon_\infty)[1 - \exp(-t/\tau_m)] \quad \text{(Eq 5)}$$

According to the above expression, the permittivity value of materials decreases when the time t is short and τ_m is large.

All these results may be directly related to the microstructure of the samples, and more particularly, to the grain size, the grain size distribution, and the density. Many studies have already been published on the size effect in ferroelectric ceramics. Kinoshita (Ref 25), and Wang et al. (Ref 26) have claimed that the finer the grain size, the higher the dielectric constant at room temperature. This is particularly true for a grain size on the order of 1 μm (the maximum being obtained for 1 μm). The value of 1 μm may be considered as an approximation of the 0.9 μm proposed by Wang, 0.8 μm proposed by Niepce et al. (Ref 27), 1 μm suggested by Duran (Ref 28) and 1.4 μm proposed by Hirata (Ref 29). This behavior is attributed to both, an increase in domain wall density and an increase in the residual internal stresses. The formation of 90° domains below T_c minimizes this internal stress energy. Nevertheless, if very small grain sizes are present (the width of the 90° domains being fixed about 1 μm in the literature) then no 90° domain may exist and, the permittivity value will decrease. This last assumption could explain the low value of the dielectric constant and the behavior observed in thick ceramics layers based on $TiCl_3$, where the grain size ranges between 0.2 and 0.5 μm. In contrast, for the thick ceramic layers based on TiO_2, since the grain size is homogenous and about 0.5-1 μm, the dielectric constant increases as the grain size increases up to 1 μm. In general, the grain size of the thick layers is smaller than that of bulk ceramics, which can be explained by the lower-sintering temperature (1200 °C for the layers versus 1250 °C for the bulk ceramics). The permittivity of the thick layers, as reported in the literature, is considerably smaller than that of bulk ceramics. This observation has often been reported, and can be explained by several factors, the most obvious being their lower density.

The bulk ceramics under study may be considered as bimodal. The observed distribution of grain sizes presents two maxima: one is centered near 0.5-1 μm for both starting powders, and the other about 10 μm ($TiCl_3$) to 50 μm (TiO_2). The value of the dielectric constant at room temperature depends on the grain size distribution (wide or narrow) and the number of small sized grains.

The difference in the Curie temperature between the different samples may also be explained by a grain size effect. As already reported by Miot (Ref 30) and Kinoshita (Ref 25), T_c increases with increasing grain-size, which is consistent with our observation that the lowest T_c is obtained for the thick layer containing the smallest grain sizes. Finally the influence of interdiffusion between the material and the electrodes on permittivity and dielectric losses measured may not be excluded.

4. Conclusion

$BaTiO_3$ powders prepared from two different titanium sources, $TiCl_3$ and TiO_2, were synthesized by hydrothermal

method. They were used to prepare ceramic pellets and thick layer samples. The two types of samples ($TiCl_3$- and TiO_2-based powders) present different microstructures and electrical properties. $BaTiO_3$ ceramic properties are dependent on the application, with mainly bimodal large angular grains growing in a fine-grained matrix with high density; whereas thick layers present a more homogenous grain size but a lower density. The difference in the distribution of the relaxation times is an electrical evidence of the differences between the two types of samples microstructures. Such differences resulting from sample preparation may be helpful when designing the devices.

The permittivity values of bulk ceramics are larger (nearly one order of magnitude) than the ones measured on thick layers. However, a value of 1000 (for TiO_2-based thick layers) may be reached. This is very promising for power electronics applications even if their maximum working frequency is about 100 kHz.

References

1. C.K. Campbell, J.D. van Wyk, and M.F. Karl Holm, Development of large-Area $BaTiO_3$ Ceramics with Optimized Depletion Regions as Dielectrics for Planar Power Electronics, *IEEE Trans. Comp. Packag. Manuf. Technol.*, 1998, **21**, p 492–499
2. P.J. Wolmarans, J.D. van-Wyk, J.D. van-Wyk Jr., and C.K. Campbell, Technology for Integrated RF-EMI Transmission Line Filters for Integrated Power Electronic Modules, *IEEE-Industry-Appl.-Conference.-37th-IAS-Annual-Meeting-Cat.-No.02CH37344.*, 2002, **3**, p 1774–1780
3. M. Boulos, S. Guillemet-Fritsch, F. Mathieu, B. Durand, T. Lebey, and V. Bley, Hydrothermal Synthesis of Nanosized BaTiO3 Powders and Dielectric Properties of Corresponding Ceramics, *Solid State Ionics*, 2005, **176**, p 1301–1309
4. S.-F. Wang, C.K. Thomas, Yang, Y.-R. Wang, and Y. Kuromitsu, Effect of Glass Composition on the Densification and Dielectric Properties of $BaTiO_3$ Ceramics, *Ceram. Int.*, 2001, **27**, p 157–162
5. M.-B. Park, S.-J. Hwang, and N.-H. Cho, Effect of the Grain Size and Chemical Feature on the Phase Transition and Physical Characteristics of Nanograined $BaTiO_3$ Ceramics, *Mater. Sci. Eng.*, 2003, **B99**, p 155–158
6. H. Xuab and L. Gaob, Hydrothermal Synthesis of High-Purity $BaTiO_3$ Powders: Control of Powder Phase and Size, Sintering Density, and Dielectric Properties, *Mater. Let.*, 2004, **58**, p 1582–1586
7. B.D. Stojanovic, C.R. Foschinic, V.Z. Pejovicd, V.B. Pavlovice, and J.A. Varelaa, Electrical Properties of Screen Printed $BaTiO_3$ Thick Films, *J. Eur. Ceram. Soc.*, 2004, **24**, p 1467–1471
8. B.D. Stojanovica, C.R. Foschinia, V.B. Pavlovicd, V.M. Pavlovice, V. Pejovicf, and J.A. Varelaa, Barium Titanate Screen-Printed Thick Films, *Ceram. Int.*, 2002, **28**, p 293–298
9. D.-H. Yoon, J. Zhang, and B.I. Lee, Dielectric Constant and Mixing Model of $BaTiO_3$ Composite Thick Films, *Mater. Res. Bull.*, 2003, **38**, p 765–772
10. B.I. Lee and J. Zhang, Dielectric Thick Films Deposition by Particle Coating Method, *Mater. Res. Bull.*, 2001, **36**, p 1065–1074
11. S. Guillemet, Th. Lebey, and F. Costa, Study of Some Ferroelectric Materials In View of Passive Components Integration in Power Electronic. *IEEE Int. Symposium Electr. Insul. Mater.*, 2001, p 823–827
12. J.C. Niepce, Diélectriques à grains très fins. In Nanomatériaux, ARAGO no 27,*OFTA Editor*, Paris, 2001, p. 149–158
13. S.W. Lu, B.I. Lee, Z.L. Wang, and W.D. Samuels, Hydrothermal Synthesis and Structural Characterization of BaTiO3 Nanocrystals, *J. Crystal Growth*, 2000, **219**, p 269–276
14. M.B. Park, S.J. Hwang, and N.H. Cho, Effect of the Grain Size and Chemical Features on the Phase Transition and Physical Characteristics Of Nano-Grained $BaTiO_3$ Ceramics, *Mater. Sci. Eng.*, 2003, **B99**, p 155
15. D.-H. Yoon and B.I. Lee, Processing of Barium Titanate Tapes with Deferent Binders for MLCC Applications—Part I: Optimization Using Design of Experiments, *J. Eur. Ceram. Soc.*, 2004, **24**, p 739–752
16. D.-H. Yoon and B.I. Lee, Processing of Barium Titanate Tapes with Deferent Binders for MLCC Applications—Part II: Comparison of the Properties, *J. Eur. Ceram. Soc.*, 2004, **24**, p 753–761
17. K.S. Cole and R.H. Cole, Dispertion and Absoption in Dielectric: I. Alternating Current Characteristics, *J. Chem. Phys.*, 1941, **9**, p 341–351
18. R. Coelho and B. Aladenize, *Les Diélectriques*. Hermès, Paris, 1993, 123–145
19. F. Bertrandias and J.P. Bertrandias, Mathématiques pour les sciences de la nature et de la vie. *Presses Universitaires de Grenoble*, 1990
20. V.V. Daniel, *Dielectric Relaxation*. Academic Press, London and New York, 1967
21. C.J.F. Butcher and P. Bordewijk, *Theory of Electric Polarization*. Elsevier, Amsterdam, 1978
22. J.R. MacDonald, *Impedance Spectroscopy, Emphasising Solid Materials and Systems*. Wiley, New York, 1987
23. J.-M. Laffargue, A. Loubiere, and A. Bui, A Characterisation Method of Varistor Degradation Based on Complex Plan Analysis CPA. *Proc. 4th International Conference on Electronic Ceramics & Applications, Aachen (Germany)*, 1994, p. 619–622
24. L.L. Hench and J.K. West, Principles of Electronic Ceramics. USA, 1990, p. 220
25. K. Kinoshita and A. Yamaji, Grain Size Effect On Dielectric Properties in Barium Titanate Ceramics, *J.Appl. Phys.*, 1976, **47**(1), p 371–373
26. X.H. Wang, R.Z. Chen, Z.L. Gui, and L.T. Li, The Grain Size Effect On Dielectric Properties of BaTiO3 Based Ceramics, *Mater. Sci. Eng.*, 2003, **B99**, p 199–202
27. N. Bernaben, A. Leriche, B. Thierry, J.C. Niepce, and R. Waser, Pure Barium Titanate Ceramics: Crystalline Structure and Dielectric Properties as a Function of Grain Size, *Fourth Eur. Ceramics*, 1995, **5**, p 203–210
28. P. Duran, D. Gutierrez, J. Tartaj, and C. Moure, Densification Behaviour, Microstructure Development and Dielectric Properties of Pure $BaTiO_3$ Prepared by Thermal Decomposition of (Ba,Ti)-Citrate Polyester Resins, *Cera. Inter*, 2002, **28**, p 283–292
29. Y. Hirata, A. Nitta, S. Sameshima, and Y. Kamino, Dielectric Properties of Barium Titanate Prepared by Hot Isostatic Pressing, *Mater. Lett.*, 1996, **29**, p 229–234
30. C. Miot, C. Proust, and E. Husson, Dense Ceramics of $BaTiO_3$, Produced from Powders Prepared by a Chemical Process, *J. Eur Cera Soc.*, 1995, **15**, p 1163–1170